

Technical report 06-021

# Model predictive control for ramp metering combined with extended Kalman filter-based traffic state estimation\*

T. Bellemans, B. De Schutter, G. Wets, and B. De Moor

*If you want to cite this report, please use the following reference instead:*

T. Bellemans, B. De Schutter, G. Wets, and B. De Moor, “Model predictive control for ramp metering combined with extended Kalman filter-based traffic state estimation,” *Proceedings of the 2006 IEEE Intelligent Transportation Systems Conference (ITSC 2006)*, Toronto, Canada, pp. 406–411, Sept. 2006.

Delft Center for Systems and Control  
Delft University of Technology  
Mekelweg 2, 2628 CD Delft  
The Netherlands  
phone: +31-15-278.24.73 (secretary)  
URL: <https://www.dsc.tudelft.nl>

---

\* This report can also be downloaded via [https://pub.bartdeschutter.org/abs/06\\_021](https://pub.bartdeschutter.org/abs/06_021)

# Model Predictive Control for Ramp Metering combined with Extended Kalman Filter-based Traffic State Estimation

Tom Bellemans, Bart De Schutter, Geert Wets and Bart De Moor

**Abstract**—Ramp metering is a dynamic traffic control measure that has proven to be very effective. There are several methods to determine appropriate ramp metering signals for a given traffic situation. In this paper, a framework consisting of model predictive control (MPC) for ramp metering, combined with extended Kalman filter-based (EKF) traffic state estimation is presented. Based on traffic measurements at a limited number of locations, the EKF is able to provide the MPC ramp metering controller with estimations of the traffic states in the motorway segments of the motorway stretch under control. By using the same traffic flow model in the EKF as in the MPC prediction model, some important model parameters of the MPC prediction model can be estimated and be fed directly to the MPC controller. This functionality enables the MPC prediction model to track changes in the traffic system (e.g. due to weather conditions, incidents, etc.). The presented EKF-MPC controller for ramp metering is simulated for a case study on the E17 motorway Ghent–Antwerp in Belgium.

**Index Terms**—Traffic flow control, ramp metering, model predictive control (MPC), extended Kalman filter (EKF)

## I. INTRODUCTION

ONE of the strategies that is used in dynamic traffic control is traffic signal control to regulate access to motorways or main roads, which is also known as ramp metering. In this paper, model predictive control (MPC) [1] is discussed as a means to determine the control signals for ramp metering set-ups. Since the MPC framework repeatedly uses a prediction model, the initial states of the prediction model need to be determined. As most of the research on traffic state estimation in the past has been based on (extended) Kalman filtering techniques [2], [3], this paper proposes an extended Kalman filtering (EKF) approach to address the estimation of the initial traffic states of the prediction model.

This paper is organized as follows. First, the general framework of MPC-based ramp metering combined with EKF is presented in Section II. In Section III, the different components of MPC-based ramp metering control are discussed. In Section IV, the EKF is discussed and it is shown how the EKF can be applied to estimate the traffic states and some parameters of the MPC prediction model. In the last section, the new EKF-MPC ramp metering

controller is simulated for a real-life situation on the E17 motorway Ghent–Antwerp in Belgium in order to investigate its performance.

## II. FRAMEWORK

The heart of the framework presented in this paper is the MPC-based ramp metering controller shown in Figure 1. In order to compute the optimal future metering rates, the MPC controller starts with the current traffic state in the network and predicts the future traffic states using the prediction model. Hence, the MPC controller needs to know the initial traffic states in the network to be able to run the prediction model. Since there are in general far more traffic states in the prediction model than there are traffic measurements available, not all traffic states are measured directly.

This problem of missing state information can be overcome by applying an EKF-based traffic state estimation. The available real-life traffic measurements are fed to the EKF, which computes the most probable values of the traffic states in the network. The metering rates, which are applied to the real-life situation are also taken into account by the EKF during the traffic state estimation (Figure 1). The EKF is discussed in more detail in Section IV.

The MPC controller uses the predicted initial traffic states to compute the control signal and apply it to the real-life traffic system. A detailed discussion of the MPC framework and of the prediction model is presented in Section III.

If the model parameters of the MPC prediction model are not updated regularly, a misfit between the behavior of the real-life network and the traffic prediction model can occur. If this misfit becomes too large, it results in a degraded performance of the MPC ramp metering controller. In the framework presented in this paper, the EKF is not only used to estimate the traffic states but it is also used to track changes of the most important model parameters of the prediction model.

The framework shown in Figure 1 is an iterative framework where the whole process is repeated at regular time intervals. Indeed, each time new traffic measurements are available, the traffic state estimation is repeated.

## III. MODEL PREDICTIVE CONTROL APPROACH TO RAMP METERING

### A. Model predictive control

This section describes how model predictive control (MPC) can be applied to ramp metering (see also [4]). The

Tom Bellemans and Geert Wets are with the Transportation Research Institute (IMOB), Hasselt University, Wetenschapspark 5 bus 6, B-3590 Diepenbeek, Belgium. email: {Tom.Bellemans, Geert.Wets}@UHasselt.be

Bart De Schutter is with the Delft Center for Systems and Control, Delft University of Technology, Mekelweg 2, 2628 CD Delft, The Netherlands, email: b.deschutter@tudelft.nl

Bart De Moor is with ESAT-SCD, Katholieke Universiteit Leuven, Kasteelpark Arenberg 10, B-3001 Leuven, Belgium. email: Bart.DeMoor@esat.kuleuven.be

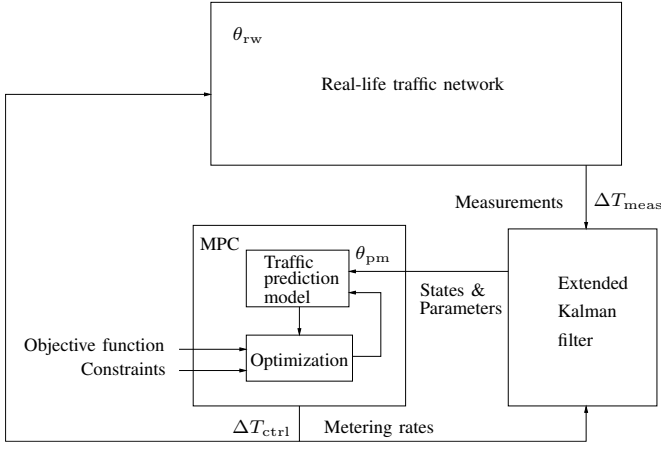


Fig. 1. Schematic representation of an EKF-MPC ramp metering controller. The EKF uses traffic measurements, which are provided at a rate  $\Delta T_{\text{meas}}$  and provides the MPC controller with estimates of the initial traffic states and with estimates of the model parameters. The rate at which the control signal is updated is  $\Delta T_{\text{ctrl}}$ .

main ingredients of MPC are that it is an on-line control approach in which a model is used to predict the future behavior of the system for a given input sequence and in which a cost criterion is optimized subject to constraints on the inputs and outputs. In addition, MPC uses a receding horizon strategy [1]. In a receding horizon framework, a prediction horizon  $N_p$  is defined and at each sample step  $k$  the metering rates for the time period  $[k\Delta T_{\text{ctrl}}, (k+N_p)\Delta T_{\text{ctrl}}]$  are determined by minimizing an objective function over this period. The controller time step  $\Delta T_{\text{ctrl}}$  is the rate at which the control signals are updated. During the optimization, the objective function, which will be discussed in detail in Section III-D, is evaluated based on a prediction of the future traffic behavior of the studied traffic system. The future traffic behavior is simulated using a traffic prediction model. An example of such a model is discussed in Section III-C.

In order to reduce the computational complexity of the optimization, the control horizon  $N_c$  ( $N_c \leq N_p$ ) is defined. The metering rate  $r(k)$  is only allowed to change during the period  $[k\Delta T_{\text{ctrl}}, (k+N_c)\Delta T_{\text{ctrl}}]$ , after which it is considered to remain constant. In a receding horizon framework, only the first calculated metering rate is applied to the ramp metering set-up. Once this metering rate is implemented, the state of the traffic in the studied area is updated using measurements, and the whole process starts all over again.

### B. Ramp metering

A ramp metering set-up consists of a traffic signal that is placed at the on-ramp of a motorway and that controls the rate at which vehicles can enter the motorway using the on-ramp. In this paper a discrete-time controller that has the metering rate as control parameter is used. The metering rate is defined as follows [5]:

$$r_o(k) = \frac{q_{\text{max},o}(k)}{Q_{\text{cap},o}}, \quad (1)$$

where  $k$  is the sample step,  $o$  is the on-ramp index,  $q_{\text{max},o}(k)$  is the maximal number of cars allowed to enter the motorway via on-ramp  $o$  during the period corresponding to sample step  $k$ , and  $Q_{\text{cap},o}$  is the capacity of on-ramp  $o$ .

When the traffic density on the motorway tends to exceed the critical density, the ramp metering set-up can limit the inflow of vehicles onto the motorway in order to keep the traffic density below the critical density, thus avoiding traffic breakdown and congestion [6]. Note that whenever the traffic demand is larger than the number of cars that is allowed to enter the motorway, a waiting queue of vehicles is formed at the on-ramp. Hence, a trade-off exists between reducing congestion on the motorway and keeping the queue length at the on-ramp below a certain level.

### C. Motorway traffic flow model

During the optimization of the metering rates over the prediction horizon, the controller uses a traffic prediction model. It is important to note that the choice of the traffic prediction model is not imposed by the MPC framework but by considerations such as accuracy and computational complexity of the model. In this section the METANET traffic flow model that will be used in the simulations for the case study discussed in Section V is presented.

The METANET model [7] is a discrete second-order macroscopic traffic flow model that represents a traffic network as a directed graph with links corresponding to motorway stretches. Each link has uniform characteristics and is subdivided in segments.

The state of segment  $i$  of link  $m$  is characterized by the traffic density  $\rho_{m,i}(l)$  (veh/lane/km), the mean speed  $v_{m,i}(l)$  (km/h), and the traffic volume or flow  $q_{m,i}(l)$  (veh/h), where the counter  $l$  corresponds to the time instant  $t = l\Delta T_{\text{sim}}$ , and where  $\Delta T_{\text{sim}}$  is the time step used for the simulation of the traffic model.

The simulation time step  $\Delta T_{\text{sim}}$  of the traffic simulation model will in general be different from the control time step  $\Delta T_{\text{ctrl}}$  and from the measurement time step  $\Delta T_{\text{meas}}$ . In order to emphasize this difference, the simulation step counter is denoted by  $l$  and the control sample counter by  $k$ . Since the measurement time step  $\Delta T_{\text{meas}}$  is chosen equal to the control time step  $\Delta T_{\text{ctrl}}$  in the simulations in Section V, the measurement sample counter is also denoted by  $k$ .

The model equations that describe the evolution of the flow, speed and density can be written down for every segment of the motorway. The first equation expresses the conservation of vehicles:

$$\rho_{m,i}(l+1) = \rho_{m,i}(l) + \frac{\Delta T_{\text{sim}}}{n_m l_{m,i}} [q_{\text{in},m,i}(l) - q_{\text{out},m,i}(l)], \quad (2)$$

where  $\rho_{m,i}(l)$  is the traffic density in segment  $i$  of link  $m$  at simulation step  $l$ ,  $q_{\text{in},m,i}(l)$  is the inflow into the segment during the time interval  $[l\Delta T_{\text{sim}}, (l+1)\Delta T_{\text{sim}}]$ ,  $q_{\text{out},m,i}(l)$  is the outflow of the segment during the same time interval, and  $n_m$  and  $l_{m,i}$  are respectively the number of lanes in link  $m$  and the length of segment  $i$  of link  $m$ .

The average speed in segment  $i$  of link  $m$  at simulation step  $l + 1$  is given by:

$$v_{m,i}(l+1) = v_{m,i}(l) + \frac{\Delta T_{\text{sim}}}{\tau_m} [V[\rho_{m,i}(l)] - v_{m,i}(l)] \\ + \frac{\Delta T_{\text{sim}}}{l_{m,i}} v_{m,i}(l) [v_{m,i-1}(l) - v_{m,i}(l)] \\ - \frac{\nu_m \Delta T_{\text{sim}} [\rho_{m,i+1}(l) - \rho_{m,i}(l)]}{\tau_m l_{m,i} [\rho_{m,i}(l) + \kappa_m]} + \xi_{m,i}^v(l), \quad (3)$$

where  $\tau_m$ ,  $\nu_m$ , and  $\kappa_m$  are link model parameters that need to be fitted to traffic data. The average equilibrium speed in a segment  $V[\rho_{m,i}(l)]$  is given by an empirical expression [8]:

$$V[\rho_{m,i}(l)] = v_{\text{free},m} \exp \left( - \frac{1}{a_m} \left( \frac{\rho_{m,i}(l)}{\rho_{\text{crit},m}} \right)^{a_m} \right), \quad (4)$$

where  $v_{\text{free},m}$  is the free flow speed of the link,  $\rho_{\text{crit},m}$  is the critical density of the link and  $a_m$  is a model parameter. In case a stochastic model is used as in Section IV,  $\xi_{m,i}^v(l)$  is the noise on the state  $v_{m,i}(l)$ . If a deterministic model is needed,  $\xi_{m,i}^v(l) = 0$  for all  $m$ ,  $i$  and  $l$ .

The traffic flow  $q_{m,i}(l)$  in segment  $i$  of link  $m$  can be expressed in terms of the traffic density and the average speed in the segment:

$$q_{m,i}(l) = \rho_{m,i}(l) v_{m,i}(l) n_m + \xi_{m,i}^q(l), \quad (5)$$

where  $\xi_{m,i}^q(l)$  is the noise on the state  $q_{m,i}(l)$  in case of a stochastic model and  $\xi_{m,i}^q(l) = 0$  for all  $m$ ,  $i$  and  $l$  in case of a deterministic model.

The splitting rate  $\beta_o(l)$  at an off-ramp  $o$  is defined as the fraction of the total traffic flow that uses the off-ramp.

When the traffic demand  $D_o(l)$  at on-ramp  $o$  exceeds the service rate  $q_{\text{on},o}(l)$  of the on-ramp, a queue is formed. The evolution of the queue length  $w_o(l)$  at on-ramp  $o$  is given by:

$$w_m(l+1) = w_m(l) + \Delta T_{\text{sim}} (D_o(l) - q_{\text{on},o}(l)). \quad (6)$$

The service rate of the on-ramp is the minimum of the number of cars that want to enter and the number of cars that can enter the motorway. This leads to the following expression:

$$q_{\text{on},o}(l) = \min \left[ D_o(l) + \frac{w_o(l)}{\Delta T_{\text{sim}}}, \right. \\ \left. Q_{\text{cap},o} \min \left( r_o(k(l)), \frac{\rho_{\text{jam},m_o} - \rho_{m_o,1}(l)}{\rho_{\text{jam},m_o} - \rho_{\text{crit},m_o}} \right) \right], \quad (7)$$

where  $Q_{\text{cap},o}$  is the capacity of the on-ramp (veh/h),  $m_o$  is the index of the link the on-ramp feeds into,  $\rho_{\text{jam},m_o}$  is the jam density of link  $m_o$  and  $k(l)$  is control sample  $k$  corresponding to simulation sample  $l$ . The service rate of the on-ramp can be limited by the metering rate  $r_o(k(l))$ .

#### D. Objective function

The MPC objective function assigns a cost to every possible traffic state on the studied motorway. The objective function used in this paper consists of the total time spent by all vehicles in the studied area and of a term that penalizes

fluctuations of the control signal. In the receding horizon framework this leads to the following expression:

$$J(k_0) = \sum_{l=l(k_0)}^{l(k_0+N_p)-1} \left[ \sum_{(m,i) \in \mathcal{I}_m} \rho_{m,i}(l) l_{m,i} n_m + \alpha_{\text{queue}} \sum_{o \in \mathcal{I}_o} w_o(l) \right] \\ + \Delta T_{\text{sim}} + \alpha_{\text{var}} \sum_{k=k_0}^{k_0+N_p-1} (r(k) - r(k-1))^2, \quad (8)$$

where  $\mathcal{I}_m$  denotes the set of all index pairs  $(i, m)$  for motorway segments, and  $\mathcal{I}_o$  is the set of all on-ramps indices. The parameter  $\alpha_{\text{queue}}$  allows to put more or less emphasis on the time spent by the vehicles in the on-ramp queue while the parameter  $\alpha_{\text{var}}$  determines the relative importance of the control smoothing term.

#### IV. EXTENDED KALMAN FILTER FOR TRAFFIC STATE AND MODEL PARAMETER ESTIMATION

The framework discussed in Section II requires the estimation of initial traffic states to be used by the MPC traffic prediction model based on limited measurements. This section describes the application of the EKF to estimate the traffic states and the model parameters for the METANET model [9].

##### A. The augmented state space model

By substituting the METANET model equations (4) and (5) in (3) and (2) respectively, two independent traffic state variables  $\rho_{m,i}(k)$  and  $v_{m,i}(k)$  are obtained that describe the traffic state in a motorway segment. Hence, the state of a motorway stretch of  $N$  segments is described by a nonlinear state space model consisting of  $2N$  equations. For convenience, the traffic states in the motorway segments are grouped in a state vector  $\mathbf{x}_1(k)$ , where  $x_{1,i}(k)$  denotes the  $i$ -th state.

At the edges of the studied motorway stretch, some boundary variables need to be determined. These boundary variables consist of the upstream traffic demand  $q_0(k)$ , the traffic demands at the on-ramps  $D_o(k)$  (if any), the splitting rates at the off-ramps  $\beta_o(k)$  (if any), the average speed in the upstream segment  $v_0(k)$  and the traffic density  $\rho_{N+1}(k)$  in the motorway segment downstream of the motorway stretch. Since the measurements of the boundary variables may be unavailable, the boundary variables are added to the state space model as a random walk process [9]:

$$x_{2,i}(k+1) = x_{2,i}(k) + \xi_{2,i}(k), \quad (9)$$

where  $x_{2,i}(k)$  denotes the  $i$ -th boundary variable and  $\xi_{2,i}(k)$  denotes the random walk state noise corresponding to the state  $x_{2,i}(k)$ . In an (extended) Kalman filter approach, all noise is considered to be zero mean Gaussian white [2].

Traffic model parameters that are expected to be subject to change over time can be incorporated in the augmented state space model as a random walk process:

$$x_{3,i}(k+1) = x_{3,i}(k) + \xi_{3,i}(k). \quad (10)$$

The standard deviation of the noise  $\xi_{3,i}(k)$  corresponding to the state  $x_{3,i}(k)$  determines the variability of the parameter in time.

The available traffic measurements are subject to measurement noise. This measurement noise can be accounted for by a measurement model. For measurements of the flow this leads to:

$$\begin{aligned} m_{m,i}^q(k) &= q_{m,i}(k) + \gamma_{m,i}^q(k) \\ &= \rho_{m,i}(k)v_{m,i}(k)n_m + \xi_{m,i}^q(k) + \gamma_{m,i}^q(k) , \end{aligned} \quad (11)$$

where  $m_{m,i}^q(k)$  denotes the average flow measurement in segment  $i$  of link  $m$  during the period  $[(k-1)\Delta T_{\text{meas}}, k\Delta T_{\text{meas}})$  and  $\gamma_{m,i}^q(k)$  denotes the corresponding flow measurement noise. In a similar way, the measurements of the average traffic speed can be modeled:

$$m_{m,i}^v(k) = v_{m,i}(k) + \gamma_{m,i}^v(k) , \quad (12)$$

where  $m_{m,i}^v(k)$  denotes the measurement of the average speed and  $\gamma_{m,i}^v(k)$  denotes the corresponding speed measurement noise.

Equations (2), (3), (4), (5), (9), (10), (11) and (12) can be summarized in the following nonlinear state space model:

$$\begin{aligned} \Sigma(\mathbf{x}, \mathbf{y}, \xi, \eta) : \quad & \mathbf{x}(k+1) = \mathbf{f}[\mathbf{x}(k), \xi(k)] \\ & \mathbf{y}(k) = \mathbf{g}[\mathbf{x}(k), \eta(k)] \end{aligned} , \quad (13)$$

where  $\mathbf{x}(k)$  is the vector with the states of the model, consisting of the traffic states  $\mathbf{x}_1(k)$ , the boundary variables  $\mathbf{x}_2(k)$ , and some important model parameters  $\mathbf{x}_3(k)$  and where  $\xi(k)$  is the state noise vector.  $\mathbf{y}(k)$  is the output vector representing the measurement model for the measured traffic flows and the measured average speeds, while  $\eta(k)$  is a noise vector consisting of state noise and measurement noise according to (11) and (12).

### B. The extended Kalman filter

Given the augmented state space model  $\Sigma(\mathbf{x}, \mathbf{y}, \xi, \eta)$ , and assuming the noise in the vectors  $\xi(k)$  and  $\eta(k)$  is zero mean Gaussian white and assuming the initial state of the system satisfies some basic conditions [9], an estimation  $\hat{\mathbf{x}}(k+1|k)$  of the next state can be found by using the EKF. The EKF tries to minimize the covariance of the estimation error:

$$E\{[\mathbf{x}(k+1) - \hat{\mathbf{x}}(k+1|k)]^T [\mathbf{x}(k+1) - \hat{\mathbf{x}}(k+1|k)]\} \quad (14)$$

by estimating the new state  $\hat{\mathbf{x}}(k+1|k)$  based on the previously predicted state  $\hat{\mathbf{x}}(k|k-1)$  and the measurements  $\mathbf{y}(k)$  according to:

$$\hat{\mathbf{x}}(k+1|k) = \mathbf{f}[\hat{\mathbf{x}}(k|k-1), \mathbf{0}] + \mathbf{K}(k)[\mathbf{y}(k) - \mathbf{g}(\hat{\mathbf{x}}(k|k-1), \mathbf{0})] . \quad (15)$$

The Kalman gain matrix  $\mathbf{K}(k)$  determines the extent to which a difference between the measured outputs  $\mathbf{y}(k)$  and the predicted outputs  $\mathbf{g}(\hat{\mathbf{x}}(k|k-1), \mathbf{0})$  leads to a correction of the estimation of the state in the next time step  $k+1$ . The Kalman gain matrix for the EKF is obtained by linearizing the nonlinear augmented state space model (13) around the previous state  $\hat{\mathbf{x}}(k|k-1)$  and solving the Riccati equation for this linearized system [9], [2].

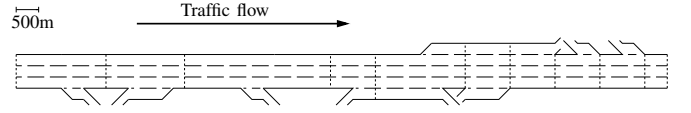


Fig. 2. Schematic representation of the stretch of the E17 motorway Ghent–Antwerp in Belgium that is considered in the case study. The vertical dashed lines denote the locations where measurements of the average speed and of the traffic flow are available.

In the next section, the EKF is applied to a real-life traffic situation where it is used to estimate the traffic states of the motorway segments and some MPC prediction model parameters based on a limited set of measurements.

## V. CASE STUDY

In this section some simulation results of the MPC-based ramp metering controller with EKF-based state estimation are presented for a real-life traffic situation in Belgium. First, the simulated motorway is presented, followed by a description of how the EKF was set-up for this simulation. Next, some simulation results regarding the estimated traffic states are presented. This section is concluded with a comparison of three control scenarios for a case study motorway: a no-control scenario, a scenario with MPC-based ramp metering assuming that all the initial traffic states required by the MPC prediction model are readily available and measured exactly, and a scenario with an MPC-based ramp metering controller with an EKF estimating the initial traffic states in the motorway segments as well as some important model parameters of the prediction model.

### A. Set-up

In this paper, a stretch of approximately 9 km of the E17 motorway Ghent–Antwerp in Belgium is considered as a case-study (Figure 2). During the morning rush hour, recurrent congestion occurs on the motorway stretch.

The available traffic measurements are updated every minute ( $\Delta T_{\text{meas}} = 1$  min) and consist of measurements of the traffic flow and the average speed at the locations indicated in Figure 2.

In order to enable the assessment of the performance of the motorway for the three scenarios that are investigated, the real-world motorway is replaced by a METANET model with a parameter set  $\theta_{\text{rw}}$  that is considered to be an exact representation of the real-world situation for this investigation. The prediction model in the MPC controller is a METANET model with a separate model parameter set  $\theta_{\text{pm}}$ .

The real-world METANET simulation model ( $\theta_{\text{rw}}$ ) is run for a morning rush hour (6 am to 11 am). The traffic demands at the mainline and at the on-ramps are assumed to be piecewise affine functions and the splitting rates are assumed to be constant. For more details on the case-study set-up the interested reader is referred to [10].

### B. Augmented traffic state model and extended Kalman filter for the case study

The motorway in Figure 2 is subdivided in 18 segments of approximately 500 m length each and  $\Delta T_{\text{sim}}$  is chosen equal

to 10 s. In order to model this motorway stretch, equations (2), (3), (4), (5) are written down for every segment. For segments with an on-ramp, equations (6) and (7) are added. As discussed in Section IV-A, the state of each segment is described by two independent state variables  $v_{m,i}(k)$  and  $\rho_{m,i}(k)$ . This yields 36 states in  $\mathbf{x}_1(k)$ .

The state vector  $\mathbf{x}_2(k)$  with the boundary variables of the motorway stretch consists of the inflow at the mainline  $q_0(k)$ , the average speed upstream of the first segment of the mainline  $v_0(k)$  and the traffic density downstream the last segment of the mainline  $\rho_{N+1}(k)$ . Additional boundary variables in  $\mathbf{x}_2(k)$  are the traffic demands  $D_1(k), \dots, D_5(k)$  at each of the on-ramps and the splitting rates  $\beta_1(k), \dots, \beta_4(k)$  for each of the off-ramps. This yields 12 states in  $\mathbf{x}_2(k)$ .

The state vector  $\mathbf{x}_3(k)$  contains the model parameters that are estimated using the EKF. All segments in between on- and off-ramps were grouped in links, resulting in 10 links (Figure 2). For each link,  $\rho_{\text{crit},m}$  is estimated using the EKF, which yields 10 states in  $\mathbf{x}_3(k)$ . The other link parameters were assumed to be known.

Hence, the augmented traffic state model has a state vector  $\mathbf{x}(k)$  with 58 states.

The output vector  $\mathbf{y}(k)$  in (13) contains 11 flow measurements and 11 accompanying average speed measurements at the locations indicated in Figure 2. These flow and speed measurements include measurements of the inflow and the average speed at the entrance of the mainline. In addition,  $\mathbf{y}(k)$  contains the inflow measurements at the on-ramps. Note that the queue dynamics, described by (6) are not incorporated in the augmented state space model. This yields an output vector  $\mathbf{y}(k)$  with 27 outputs.

The behavior of the EKF can be tuned by choosing the assumed standard deviation (SD) for the noise of each state or output appropriately. The standard deviations on the state noises were chosen as follows:  $\text{SD}(\xi^{q_{m,i}}) = 100$  veh/h,  $\text{SD}(\xi^{v_{m,i}}) = 11$  km/h,  $\text{SD}(\xi^{q_0}) = 10$  veh/h,  $\text{SD}(\xi^{v_0}) = 1$  km/h,  $\text{SD}(\xi^{\rho_{N+1}}) = 1.5$  veh/km/lane,  $\text{SD}(\xi^{D_j}) = 3$  veh/h (with  $j = 1, \dots, 5$ ),  $\text{SD}(\xi^{\beta_j}) = 0.001$  (with  $j = 1, \dots, 4$ ) and  $\text{SD}(\xi^{\rho_{\text{crit},m}}) = 0.5$  veh/km/lane.

The standard deviations on the measurement noise on the outputs were chosen as follows:  $\text{SD}(\eta^{q_j}) = 100$  veh/h and  $\text{SD}(\eta^{v_j}) = 11$  km/h (with  $j = 1, \dots, 11$ ),  $\text{SD}(\eta^{q_0}) = 5$  veh/h,  $\text{SD}(\eta^{v_0}) = 5$  km/h and  $\text{SD}(\eta^{D_j}) = 5$  veh/h (with  $j = 1, \dots, 5$ ).

### C. Extended Kalman filter simulation results

In order to evaluate the sensitivity of the EKF to the choice of the initial states of the augmented model, several simulations were conducted with different sets of initial states. Initial values that were tested were: 75%, 90% and 110% of the values of the corresponding states and parameters in the real-world model ( $\theta_{\text{rw}}$ ). In each case, the EKF converged to the correct values. For the remainder of the simulations, the initial values of the states of the augmented traffic state model were chosen equal to 90% of their real corresponding values.

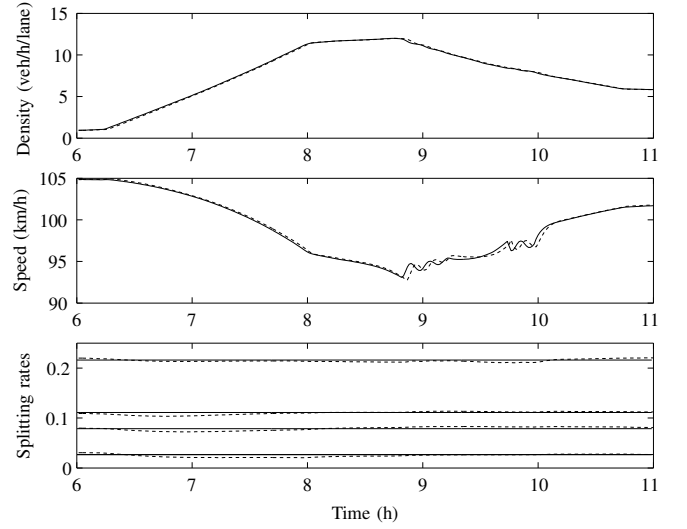


Fig. 3. The evolution of the density (top) and the average speed (middle) in a link between the third on-ramp and the fourth off-ramp. The bottom figure presents the splitting rates at the off-ramps. The solid lines represent the real-world values, while the dashed lines represent the EKF-based estimations.

A burn-in period was implemented in the simulations in order to allow the EKF to converge after starting up with the initial state values [11]. The burn-in period consisted of five times the simulated morning rush hour (25h) and the presented simulation results are the results of the sixth period.

Figure 3 shows the evolution of the traffic density and the average speed in a segment located between the third on-ramp and the fourth off-ramp. Although the traffic states of this segment are not measured directly, there is only minimal difference between the traffic states in the real-world (model with parameter set  $\theta_{\text{rw}}$ ) and the traffic states estimated by the EKF. The splitting rates, which are boundary values that are not measured in this case study, are provided by the EKF as well (Figure 3, bottom).

### D. Simulation of the EKF-MPC controller for ramp metering

To conclude the case study simulation, a comparison is made between three scenarios: a simulation without control, a simulation with MPC-based ramp metering under the assumption that the traffic states in the real world are all known by the prediction model of the MPC controller and a simulation of MPC-based ramp metering with EKF-based state estimation.

In this paper the following tuning parameters were chosen for the MPC-based ramp metering controller:  $\Delta T_{\text{ctrl}} = 1$  min, a prediction horizon of 10 minutes ( $N_p = 10$ ), a control horizon of 5 minutes ( $N_c = 5$ ),  $\alpha_{\text{var}} = 40$  and  $\alpha_{\text{queue}} = 1$ . The tuning of these parameters is discussed in more detail in [4]. Ramp metering was implemented at the fourth on-ramp (Figure 2).

In order to assess the performance of the traffic operation in each of the above scenarios, the total time spent (TTS) by all of the vehicles on the motorway and in the queues at the on-ramps was computed. In the case without control, the TTS

was found to be equal to 2038 veh.h. If the MPC prediction model is fed with the exact initial traffic states of all the segments, MPC-based ramp metering control at the fourth on-ramp yields a TTS of 1911 veh.h. If the MPC-based ramp metering controller is set-up in combination with an EKF-based traffic state and MPC prediction model parameter estimation, the TTS in the network is 1913 veh.h.

The application of the framework presented in Section II to the case study leads to an EKF-MPC ramp metering controller, which does not need detailed measurements of each segment state. Indeed, in case sufficient traffic measurements are available in the studied area [9], the EKF is able to compute a state and parameter estimation for the MPC prediction model such that the EKF-MPC ramp metering controller performs as well as an MPC ramp metering controller with complete knowledge of all initial states. This allows for the real-life implementation of the EKF-MPC ramp metering controller since in practice, only a limited number of measurements is available.

In Figure 4, the metering rate and the queue length at the fourth on-ramp are shown for both MPC-based controllers. As can be observed in the upper graph, the metering rate computed by the MPC controller with complete knowledge of the traffic states behaves smoother than the metering rate computed by the EKF-MPC controller. However, this less smooth behavior hardly harms the performance of the controller in terms of TTS. If desired, the metering rate can be smoothed by increasing the value of  $\alpha_{\text{var}}$ , which penalizes variations in the control signal. It was found [4] that the value of  $\alpha_{\text{var}}$  can be strongly increased before the controller performance starts to degrade.

The second graph in Figure 4 illustrates that the evolution of the queue length is similar for both controllers and that both controllers are able to honor the queue length constraint of 100 vehicles.

The average speed and the traffic density vary slightly more over time in the case of EKF-MPC ramp metering controller (Figure 4). However, the oscillations in the traffic state can be suppressed by increasing  $\alpha_{\text{var}}$ .

## VI. CONCLUSIONS

In this paper a framework in which MPC-based ramp metering is combined with EKF-based state estimation was presented. The EKF was used to estimate the initial traffic states of the motorway segments in the MPC prediction model, although not all of these states are measured in practice. It was shown in a simulation example of a real-life case study that the EKF is able to estimate the traffic states of the segments with such accuracy that the performance of the resulting EKF-MPC ramp metering controller is similar to the performance of the MPC controller with perfect knowledge of the initial traffic states. Besides the estimation of the traffic states, the EKF approach was also used to estimate the most important parameters of the MPC prediction model ( $\rho_{\text{crit},m}$ ) in order to reduce the misfit between the situation in real-life and the MPC prediction model.

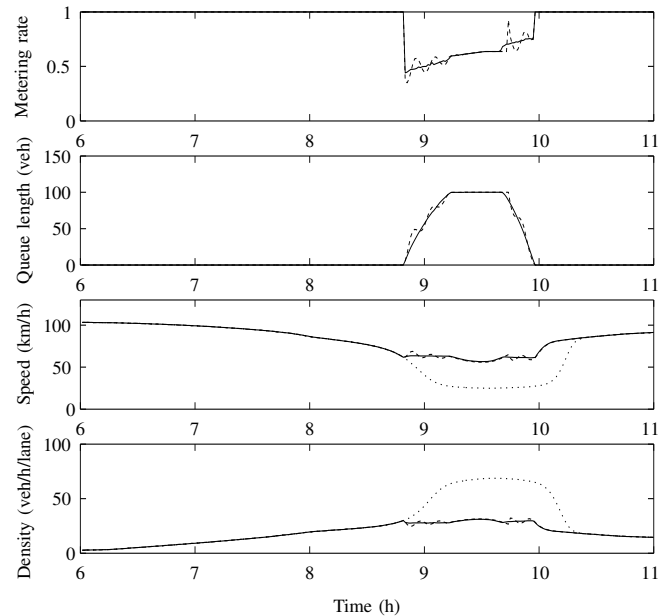


Fig. 4. Evolution of the metering rate, the queue length, the average speed and the traffic density in the segment at the fourth on-ramp. The solid lines represent the simulation results for the MPC controller with exact values of the initial states and MPC prediction model parameters, the dashed line represents the simulation results for the MPC controller combined with EKF-based state and parameter estimation. The dotted line represents the no-control scenario (metering rate = 1 and queue length = 0 veh).

## REFERENCES

- [1] J. Maciejowski, *Predictive Control with Constraints*. Harlow, England: Prentice Hall, 2002.
- [2] R. E. Kalman and R. S. Bucy, "New results in linear filtering and prediction theory," in *Trans. ASME series D*, vol. 83, 1961, pp. 95–108.
- [3] A. H. Jazwinsky, *Stochastic Processes and Filtering Theory*. New York: Academic Press, 1970.
- [4] T. Bellemans, B. De Schutter, and B. De Moor, "Model predictive control for ramp metering of motorway traffic: A case study," *Control Engineering Practice*, vol. 14, no. 7, pp. 721–852, July 2006.
- [5] A. Kotsialos, M. Papageorgiou, M. Mangeas, and H. Haj-Salem, "Coordinated and integrated control of motorway networks via non-linear optimal control," *Transportation Research Part C*, vol. 10, no. 1, pp. 65–84, Feb. 2002.
- [6] H. Zhang, S. Ritchie, and W. Recker, "Some general results on the optimal ramp control problem," *Transportation Research Part C*, vol. 4, no. 2, pp. 51–69, 1996.
- [7] M. Papageorgiou, J. Blosseville, and H. Haj-Salem, "Modelling and real-time control of traffic flow on the southern part of Boulevard Périphérique in Paris: Part I: Modelling," *Transportation Research Part A*, vol. 24, no. 5, pp. 345–359, Sept. 1990.
- [8] A. May, *Traffic Flow Fundamentals*. Englewood Cliffs, New Jersey: Prentice-Hall, 1990.
- [9] Y. Wang and M. Papageorgiou, "Real-time freeway traffic state estimation based on extended kalman filter: A general approach," *Transportation Research B*, vol. 39, pp. 141–167, Feb. 2005.
- [10] T. Bellemans, "Traffic control on motorways," Ph.D. dissertation, Katholieke Universiteit Leuven, Leuven, Belgium, 2003, available by ftp from <ftp://ftp.esat.kuleuven.be/pub/SISTA/bellemans/PhD/03-82.pdf>.
- [11] Y. Wang, M. Papageorgiou, and A. Messmer, "An adaptive freeway traffic state estimator and its real data testing - part i: Basic properties," in *Transactions of the 2005 IEEE Intelligent Transportation Systems and Control (ITSC) conference*, 2005, pp. 531–536.